

Effective Supersymmetry at the LHC

Howard Baer^{1*}, Sabine Kraml^{2†}, Andre Lessa^{1‡},
Sezen Sekmen^{3§} and Xerxes Tata^{4,5¶}

¹*Dept. of Physics and Astronomy, University of Oklahoma, Norman, OK 73019, USA*

²*Laboratoire de Physique Subatomique et de Cosmologie, UJF Grenoble 1, CNRS/IN2P3, INPG, 53 Avenue des Martyrs, F-38026 Grenoble, France*

³*Dept. of Physics, Florida State University, Tallahassee, FL 32306, USA*

⁴*Dept. of Physics and Astronomy, University of Hawaii, Honolulu, HI 96822, USA*

⁵*Dept. of Physics, University of Wisconsin, Madison, WI 53706, USA*

Abstract

We investigate the phenomenology of Effective Supersymmetry (ESUSY) models wherein electroweak gauginos and third generation scalars have masses up to about 1 TeV while first and second generation scalars lie in the multi-TeV range. Such models ameliorate the SUSY flavor and CP problems via a decoupling solution, while at the same time maintaining naturalness. In our analysis, we assume independent GUT scale mass parameters for third and first/second generation scalars and for the Higgs scalars, in addition to $m_{1/2}$, $\tan\beta$ and A_0 , and require radiative electroweak symmetry breaking as usual. We analyse the parameter space which is consistent with current constraints, by means of a Markov Chain Monte Carlo scan. The lightest MSSM particle (LMP) is mostly, but not always the lightest neutralino, and moreover, the thermal relic density of the neutralino LMP is frequently very large. These models may phenomenologically be perfectly viable if the LMP before nucleosynthesis decays into the axino plus SM particles. Dark matter is then an axion/axino mixture. At the LHC, the most important production mechanisms are gluino production (for $m_{1/2} \lesssim 700$ GeV) and third generation squark production, while SUSY events rich in b -jets are the hallmark of the ESUSY scenario. We present a set of ESUSY benchmark points with characteristic features and discuss their LHC phenomenology.

PACS numbers: 14.80.Ly, 12.60.Jv, 11.30.Pb

*Email: baer@nhn.ou.edu

†Email: sabine.kraml@lpsc.in2p3.fr

‡Email: lessa@nhn.ou.edu

§Email: sezen.sekmen@cern.ch

¶Email: tata@phys.hawaii.edu

1 Introduction

Particle physics models that include weak scale softly broken supersymmetry (SUSY) are especially compelling in that they stabilize the weak scale, even in the presence of new physics at much higher energy scales, such as M_{Planck} or M_{GUT} . The simplest of such models, the Minimal Supersymmetric Standard Model (MSSM) [1, 2] enjoys some compelling indirect experimental support in that the measured values of the gauge couplings at energy scale $Q = M_Z$, when run to high energies via renormalization group evolution (RGE), nearly unify at $Q = M_{\text{GUT}} \simeq 2 \times 10^{16}$ GeV, as is expected in the simplest grand unified theories (GUTs). On the astrophysical side, SUSY theories with a conserved R -parity offer several candidates for the dark matter particle, among these: the lightest neutralino, the gravitino and the axion/axino supermultiplet.

Along with these successes, *generic* SUSY models also lead to new puzzles not present in the Standard Model (SM). Additional (usually discrete) symmetries are necessary to prevent a too rapid rate for proton decay. Moreover, unless weak scale soft SUSY breaking (SSB) parameters of the MSSM are flavor-blind [1] or “aligned” [3], and nearly real, the model leads to unacceptably large rates for flavor-changing transitions and CP violating effects. We stress that various (sometimes, admittedly *ad hoc*) mechanisms have been suggested to ameliorate these undesired effects which, we speculate, arise because of our lack of understanding of how SM superpartners feel the effects of SUSY breaking.

Another possibility to suppress unwanted flavor-changing and CP -violating effects is to arrange for matter particles to be heavy so that their effects are sufficiently suppressed [4]. Large matter scalar masses also serve to suppress proton decay processes in a SUSY GUT. This *decoupling solution* to the SUSY flavor problem usually requires SSB terms of order 10–100 TeV [5], well beyond expectations from naturalness, which favors weak scale soft terms. It was noted as far back as 1986 [6], and later again in Ref. [7], that the stability of the weak scale to radiative corrections requires only the electroweak (EW) gauginos and third generation particles — these couple with large strength to the Higgs sector — to have masses up to $\mathcal{O}(1)$ TeV, while gluinos and superpartners of the first two generations (whose direct couplings to the Higgs sector are very small, so that these enter naturalness considerations only at the two-loop level) could well have multi-TeV masses. Since the most stringent constraints on flavour- and CP -violation come from the first two generations of quarks and leptons, such a mass spectrum potentially alleviates the SUSY flavor and CP problems without the need for undue fine-tuning of parameters. This was subsequently developed into the framework referred to as “Effective Supersymmetry” (ESUSY), by Cohen, Kaplan and Nelson [8], who suggested two different realizations of the split matter generations idea by introducing a SUSY-breaking sector to which the first two generations couple more strongly than the third generation. As a result, the matter scalars of the first two generations acquire larger SUSY-breaking masses than third generation scalars.

The ESUSY scenario seems in recent years to have become less favored due to two measurements. The first — the measured $(2-3)\sigma$ deviation in $(g-2)_\mu$ from its Standard Model (SM) expectation [9] — seems to require smuons/muon sneutrinos in the sub-TeV range if the deviation is to be attributed to SUSY. The second — the increasingly precise measurement of the dark matter (DM) density of the Universe — is difficult to reconcile in ESUSY if the

dark matter is assumed to be dominantly composed of thermal relic neutralinos left over in standard Big Bang cosmology. With scalars in the multi-TeV range, along with a bino-like neutralino, the relic density is calculated to be typically several orders of magnitude higher than the experimentally observed value [10],

$$\Omega_{\text{DM}}h^2 = 0.1123 \pm 0.0035, \quad (1)$$

although there are some special parameter regions where this need not be the case.

At the present time, it is not completely clear whether the $(g-2)_\mu$ anomaly is real. The current discrepancy arises if one adopts the (more direct to use) hadronic vacuum polarization amplitude from low energy $e^+e^- \rightarrow \text{hadrons}$ data. If instead the vacuum polarization is taken from τ lepton decay data, then the discrepancy is smaller (but recently growing!).

In the case of neutralino DM, it is possible to have a small superpotential μ term co-existing with large scale masses, as occurs *e.g.* in the hyperbolic branch/focus point region of the mSUGRA¹ model. Then the lightest neutralino, instead of being typically bino-like with a small annihilation cross section and concomitantly large relic density, becomes mixed higgsino dark matter with thermal relic neutralinos from the Big Bang making up the observed cold dark matter relic density. Other possibilities for obtaining the right relic density are resonant annihilation through the pseudoscalar Higgs, or co-annihilation with third-generation sfermions.

Regions of parameter space where the neutralino relic density is too large cannot be unequivocally excluded in extensions of the model. For instance, if one invokes the Peccei-Quinn-Weinberg-Wilczek (PQWW) solution to the strong CP problem [11], then one expects the presence of an axion/axino supermultiplet in SUSY theories. If the axino \tilde{a} is the lightest SUSY particle (LSP), then $\tilde{Z}_1 \rightarrow \tilde{a}\gamma$ and other decay modes are allowed, which can greatly reduce the DM abundance far below the level expected from neutralinos. The scenario of mixed axion/axino DM has been examined in the SUGRA context recently in Ref. [12] in a general 19 parameter MSSM, and appears to be at least as viable as the case with neutralino DM.

In light of these considerations, we feel it would be fruitful to re-visit some of the phenomenological implications of ESUSY models at the beginning of the LHC era. In our analysis, we subsume the qualitative features of the ESUSY model: *i.e.* third generation, Higgs sector and EW gaugino masses at or below the TeV scale, with multi-TeV SSB parameters for the first two generations. For simplicity we also assume gaugino mass unification.² While we adopt the qualitative picture of Effective SUSY, we do *not* assume the validity of the more speculative mechanisms that the authors of Ref. [8] suggest for the hierarchy between the SSB parameters of the first two generations and the corresponding parameters for the third generation and the gaugino sector. For our phenomenological analysis, we simply assume that such a hierarchy occurs for SSB parameters renormalized at a high scale that we take to be M_{GUT} . We also take the less ambitious view that the SUSY flavour and CP problems are ameliorated, but not completely solved, by this hierarchy, and allow the first two generations of scalars to have masses in the 5–20 TeV range, so that some degree of universality/alignment (for the first two

¹Minimal Supersymmetric model with Universal soft terms at the Gut scale and RAdiative electroweak symmetry breaking.

²While the gluino mass parameter can, in principle, be hierarchically larger, RGE effects due to a very heavy gluino would raise third generation squark mass parameters to high values. Gauge coupling unification also prefers that the gluino not be too heavy.

generations) is still necessary to satisfy the most stringent flavour constraints. For simplicity, we will assume GUT scale scalar mass universality in the subspace of the first two generations, but allow independent SSB parameters for the third generation and the Higgs sector. This assumption of diagonal GUT scale scalar SSB mass squared matrices undoubtedly has an effect on flavor physics [13], but should have very limited impact on the implications for collider physics and cosmology of the ESUSY scenario — which are after all our main interest in this paper.

The ESUSY model parameter space we will examine is thus given by the set of parameters (renormalized at the GUT scale)

$$m_0(1, 2), m_0(3), m_{H_u}, m_{H_d}, A_0, m_{1/2}, \tan \beta, \text{sign}(\mu) \quad (2)$$

along with the top quark mass $m_t = 173.1 \pm 1.3$ GeV. Here $m_0(1, 2)$ and $m_0(3)$ are the masses of the first/second and of the third generation sfermions, respectively; $m_{H_u} \equiv m_{H_u}^2 / \sqrt{|m_{H_u}^2|}$ and $m_{H_d} \equiv m_{H_d}^2 / \sqrt{|m_{H_d}^2|}$, are the SSB mass parameters of the up- and down-type Higgs scalars; A_0 is a universal trilinear coupling (relevant mostly only for the third generation); $m_{1/2}$ a universal gaugino mass parameter; and $\tan \beta \equiv v_u/v_d$. Radiative electroweak symmetry breaking can be used to determine μ^2 using the measured value of M_Z .

We wish to maintain the successful gauge coupling unification at $Q = M_{\text{GUT}}$, so that we will assume here that the MSSM is the correct effective field theory between M_{GUT} and $\widetilde{M} = m_0(1, 2)$, the scale at which first and second generation scalars decouple from the theory. Below \widetilde{M} , we have ESUSY — the SM with two Higgs boson doublets together with third generation scalars, gauginos and higgsinos — as the effective theory.

Models with third generation scalar and gaugino-higgsino sector at \lesssim TeV but multi-TeV first and second generation mass parameters have been investigated in the past. Shortly after Cohen *et al.* [8] laid down their framework, it was noted that two loop RGE effects arising due to heavy first/second generation scalars act to suppress third generation scalar mass parameters (even to tachyonic values), and a variety of flavor and CP -violating constraints were examined [5, 14]. In Refs. [15, 16] it was shown that the inverted scalar mass hierarchy which is the hallmark of the ESUSY scenario could emerge dynamically in models with Yukawa coupling unification, although the $\widetilde{M} : M_{\text{weak}}$ ratio was found to be limited [16]. This class of models — requiring $t - b - \tau$ Yukawa coupling unification and $SO(10)$ like boundary conditions with $\tan \beta \sim 50$ — has been investigated in detail in Refs. [17, 18]. In Ref. [19], the magnitude of the $\widetilde{M} : M_{\text{weak}}$ hierarchy was investigated in models without Yukawa coupling unification where the matter scalar mass parameters are already taken to be split at the GUT scale. This study assumed equal GUT scale values of third generation and Higgs SSB masses, and as a result, was limited in scope compared to the results to be presented here. In addition, several authors have investigated other related aspects of supersymmetric models with heavy scalars [20].

The remainder of this paper is organized as follows. In Sec. 2, we explore the parameter space in Eq. (2) and map out ranges of parameters that potentially lead to ESUSY at the weak scale. In Sec. 3, we perform a Markov Chain Monte Carlo (MCMC) analysis to search for SUSY scenarios which fulfill the ESUSY conditions, subject to various experimental constraints. We first describe the setup of our MCMC, and then show results for posterior probability

distributions both for input parameters that result in ESUSY, as well as for expectations for various particle masses and selected experimental observables. Moreover, we pick out some characteristic benchmark points for further study. In Sec. 4, we first present the main particle production rates and decay patterns relevant for LHC phenomenology of the ESUSY scenarios, and then illustrate the diversity of LHC phenomena through more detailed discussion of the phenomenology of the benchmark points, including the possibility that the lightest MSSM sparticle (LMP, as distinct from LSP) may be charged or coloured. We conclude in Sec. 5 with a summary of our results.

2 Viable spectra and parameter space of the ESUSY model

Constrained supersymmetric models such as the mSUGRA model have, for a fixed gluino mass, an upper limit on how massive scalars can be. For a model with universal scalar mass soft terms at the GUT scale, given by m_0 , with $m_{1/2}$ fixed, the weak scale value of μ^2 diminishes as m_0 increases. Ultimately, when m_0 is large enough, $|\mu|$ becomes comparable to the weak scale value of the bino mass M_1 , and one gains neutralinos of mixed higgsino-bino composition which make a good candidate for thermal WIMPs. This is the so-called hyperbolic branch/focus point (HB/FP) region of the SUGRA parameter space [21]. As m_0 increases even further, $|\mu|$ decreases even more and the \tilde{Z}_1 becomes nearly pure higgsino, and the higgsino-like lightest chargino may drop below limits from LEP2 searches. For yet higher values of m_0 , μ^2 becomes negative, signaling an inappropriate electroweak symmetry breaking (EWSB) pattern. Thus, in the mSUGRA model, for a given value of $m_{1/2}$, m_0 can become no larger than a few TeV.

If we proceed to models with non-universal generations, taking $m_0(1, 2)$ as independent of $m_0(3)$, with $m_0(3) = m_{H_u} = m_{H_d} \equiv m_H$ as in Ref. [19], we expect, using 1-loop RGEs, by the same reasoning, an upper bound on $m_0(3)$. The point is that the first and second generations essentially decouple from the RG evolution of the Higgs SSB parameters (which enter the electroweak potential minimization conditions, see Ref. [22]). At two loop order, however, very large scalar masses do affect the running of the other scalar masses and in fact lead to their suppression at the weak scale [14, 19]. As $m_0(3)$ decreases (or $m_0(1, 2)$ increases), so $m_0(3) \ll m_0(1, 2)$, one of the third generation scalars becomes the LSP, turning tachyonic for even smaller (larger) $m_0(3)$ ($m_0(1, 2)$) values. Therefore, with $m_0^2(3) = m_{H_{u,d}}^2$ at the GUT scale, there are both an upper (from $\mu^2 > 0$) and a lower (from $m_{\tilde{t},\tilde{b},\tilde{\tau}}^2 > 0$) bound on $m_0(3)$. In Fig. 1, we show regions of allowed parameter space in the m_H versus $m_0(3)$ plane for $m_0(1, 2) = 5, 10$ and 20 TeV, with *a*) $m_{1/2} = 300$ GeV and *b*) $m_{1/2} = 800$ GeV, where the spectrum calculations are performed using `Isajet7.80` [23]. The green dashed line is where $m_H \equiv m_0(3)$. The region to the right of the blue lines is forbidden due to lack of EWSB, while the region below the red lines is forbidden because a third generation scalar becomes tachyonic. The region to the left and above the contours yields viable spectra.

For low $m_{1/2}$, we see from Fig. 1*a*) that if we restrict our attention to $m_H = m_0(3)$ (green dashed line) only the interval $1 \text{ TeV} \lesssim m_0(3) = m_H \lesssim 4 \text{ TeV}$ is allowed for $m_0(1, 2) = 5$ TeV, while there are no allowed values for $m_0(1, 2) = 10$ or 20 TeV, since for these cases the

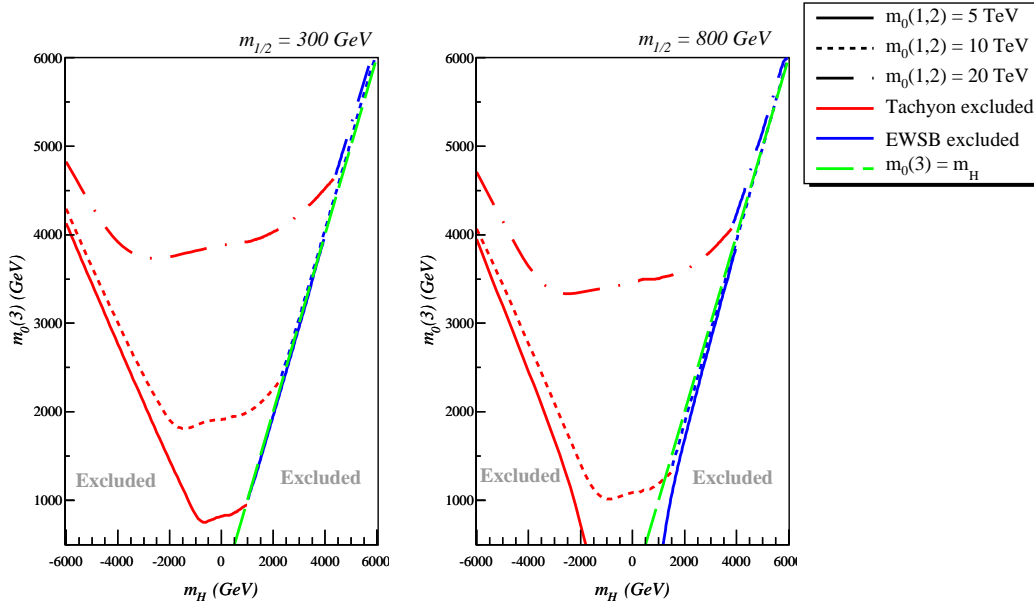


Figure 1: *Regions of parameter space leading to viable sparticle mass spectra in the m_H vs. $m_0(3)$ plane for $m_0(1,2) = 5, 10$ and 20 TeV. We fix $A_0 = 0$, $\tan\beta = 10$ and $\mu > 0$ and choose $m_{1/2} = 300$ GeV in the left frame and $m_{1/2} = 800$ GeV in the right frame. The region below the red lines is excluded because of tachyonic third generation masses or, for large negative values of m_H because $m_A^2 < 0$, while the region to the right of the blue lines does not allow EWSB. The green dashed line has $m_0(3) = m_H$. The ESUSY spectra results from taking $m_0(3)$ to its lowest allowed values.*

$m_0(3) = m_H$ line lies entirely in the excluded region. However, through 1-loop RGE running effects, an increase in $m_{1/2}$ increases $m_{\tilde{q}}$. Hence larger values of $m_0(1,2)$ become viable if $m_{1/2}$ is large enough. This is seen in Fig. 1b), where the green dashed line (again representing $m_0(3) = m_H$) shows that, for $m_{1/2} = 800$ GeV, the range of allowed $m_0(3) = m_H$ values is larger for $m_0(1,2) = 5$ TeV, where the tachyonic lower bound is gone, so $0 < m_0(3) = m_H \lesssim 5$ TeV. Besides, if a neutralino LSP is required, we have $0.25 < m_0(3) = m_H \lesssim 5$ TeV. For the higher $m_0(1,2)$ cases we see that the increase in $m_{1/2}$ provides an allowed region for $m_0(1,2) = 10$ TeV, but still is insufficient for the $m_0(1,2) = 20$ TeV case. It is for this reason that the solutions found in Ref. [19] with very large $m_0(1,2)$ values, as needed to suppress FCNCs, also required rather high $m_{1/2}$ values, and consequently very heavy gluinos: quite beyond the reach of LHC.

Since there is no compelling theoretical argument to link the Higgs and third generation mass scales, it seems reasonable to adopt independent values of $m_0(3)$ and $m_{H_u} = m_{H_d} = m_H$ (NUHM1) or $m_{H_u} \neq m_{H_d}$ (NUHM2). In this case, for a large value of $m_0(3)$, we can take $m_H^2 \ll m_0^2(3)$, and thus give m_H a head start on running towards the necessary negative squared values which are needed for successful EWSB (recall that at the weak scale, $\mu^2 \simeq -m_{H_u}^2$ for even modest values of $\tan\beta$). This is the well-known feature of NUHM1 models wherein increasing m_H results in a decrease of the weak scale value of $|\mu|$ [24]. Note that large negative values of m_H are excluded because there $m_A^2 < 0$, signaling that EWSB is not correctly obtained.

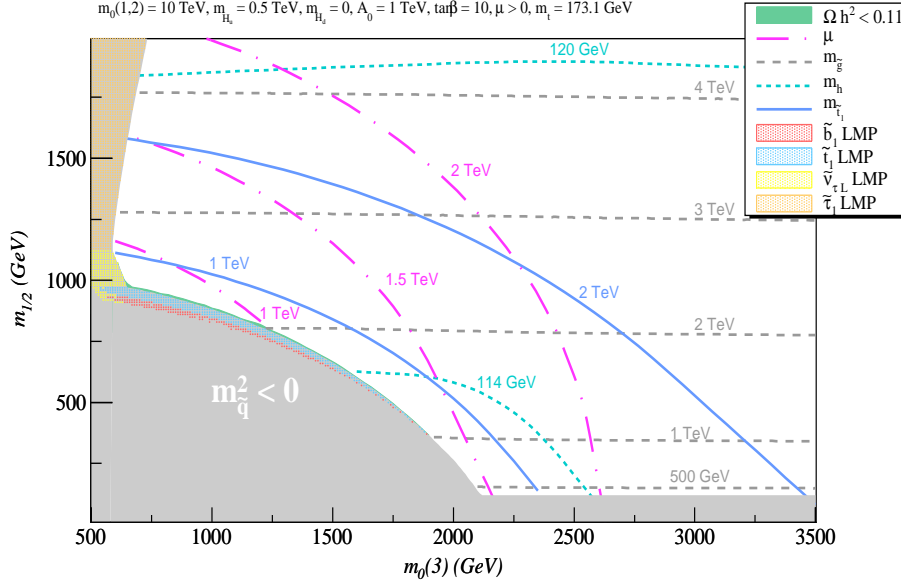


Figure 2: Contours of μ , gluino, stop and Higgs (h) boson masses in the $m_0(3)$ vs. $m_{1/2}$ plane for $m_0(1,2) = 10$ TeV, $m_{H_u} = 0.5$ TeV, $m_{H_d} = 0$, $A_0 = 1$ TeV, $\tan\beta = 10$ and $\mu > 0$. Also shown are regions where various scalars are the lightest MSSM particles (LMPs). In the almost impossible to see narrow green band whose thickness is $\lesssim 10$ GeV that hugs the upper boundary of the stop LMP region, the thermal relic abundance $\Omega_{\tilde{Z}_1} h^2 < 0.11$. The gray shaded region is excluded because either we have tachyonic sparticles or the chargino mass is below the corresponding LEP2 limit.

If we adopt a low value of $|m_H| \lesssim 1$ TeV, and then move from high to low $m_0(3)$ values, the third generation scalars decrease in mass. The region for ESUSY with third generation scalars at \lesssim TeV is at $m_0(3)$ values just above the tachyonic third generation region. Thus, the strategy for gaining viable ESUSY spectra is to 1.) adopt a large value of $m_0(1,2) \sim 5 - 20$ TeV, then 2.) adopt a low value of $m_H \sim 0 - 2$ TeV, and finally, 3.) starting at a several TeV value of $m_0(3)$, decrease its value until third generation scalars dip below the TeV region. If we want low $|\mu|$ values as well, then increase m_H as close to the EWSB boundary (on the right of the figure) as desired.

It is instructive to portray ESUSY in various parameter planes. Figure 2 shows the allowed region in the $m_0(3)$ vs. $m_{1/2}$ plane with $m_0(1,2) = 10$ TeV, $m_{H_u} = 0.5$ TeV, $m_{H_d} = 0$ TeV (along with $A_0 = 1$ TeV, $\tan\beta = 10$ and $\mu > 0$). The left-side gray shaded region gives tachyonic stop or sbottom masses, while in the lower-right gray region the chargino mass is below its LEP2 limit. The white region gives viable supersymmetric mass spectra. We plot contours of $m_{\tilde{g}}$ (gray dashed), $m_{\tilde{t}_1}$ (blue solid), m_h (dashed cyan) and μ (magenta dot-dashed). The region to the lower left of the cyan dashed contour has $m_h < 114$ GeV. The slim region adjacent to but right of the tachyonic stop region gives viable ESUSY spectra with top squark masses $m_{\tilde{t}_1} < 1$ TeV. There is an almost-impossible-to-see green region of thickness $\lesssim 6$ GeV in $m_{1/2}$ hugging the boundary of the tachyonic stop region where the thermal neutralino abundance is in accord

with measurement: $\Omega_{\tilde{Z}_1} h^2 < 0.11$. This is, in fact, the top squark co-annihilation region [25] for ESUSY. Along the tachyonic boundary is another narrow region where the \tilde{t}_1 can become the lightest MSSM particle (LMP), though not necessarily the LSP if a non-MSSM R -odd sparticle (such as the axino) is lighter. We also show the regions where \tilde{b}_1 , $\tilde{\tau}_1$ or $\tilde{\nu}_{\tau L}$ is the LMP.³

In Fig. 3a), we fix instead the values of $m_0(1, 2)$, $m_0(3)$ and $m_{1/2}$ and plot contours of $m_{\tilde{t}_1}$, μ and m_A in the m_{H_u} vs. m_{H_d} plane. As discussed above, for intermediate positive ranges of m_{H_d} in the plot, where $m_{H_u} \sim m_{H_d}$, as m_{H_u} increases, the value of μ decreases until $\mu^2 < 0$ and EWSB is no longer realized. This can be seen by the μ contours in this part of the figure where we also see a significant green region where the thermal neutralino relic density is consistent with its observed value. In the lower portion (low m_{H_d}) of the grey area on the right and at the bottom in Fig. 3a), we do not obtain radiative EWSB because m_h^2 or m_A^2 become negative. The green region in this vicinity is where the neutralino relic density is compatible because of higgs resonance annihilation [26]. Finally, for large enough positive values of m_{H_u} and m_{H_d} , \tilde{t}_1 becomes the LMP (shaded blue region), with $m_{\tilde{t}}^2 < 0$ above that (upper portion of the grey area on the right) and co-annihilation with stops leads to a compatible neutralino relic density. Finally, we present in Fig. 3b) the allowed region in the m_{H_u} vs. $m_0(3)$ plane with $m_0(1, 2) = 10$ TeV, $m_{1/2} = 0.5$ TeV and $m_{H_d} = 1$ TeV. We see that the ESUSY scenario is realized at low $m_0(3)$ and $m_{H_u} \lesssim m_0(3)$.

3 Markov Chain Monte Carlo analysis of ESUSY

In this section, we perform an MCMC analysis to map out the regions of ESUSY parameter space that are consistent with current experimental constraints from collider and flavour physics. The characteristics of ESUSY are enforced by means of theoretical priors. We first briefly describe our set up and list the likelihood functions and model priors that we use, and then show our results for the posterior probability distributions both for input parameters as well as various sparticle masses and selected experimental observables. In Sec. 3.3, we present some benchmark points for more detailed study.

3.1 Setup of the MCMC scans

The setup and procedure of our MCMC closely follow [27], so we do not repeat these here but instead just give the key data of the analysis. For details on the MCMC method and Bayesian analysis, see *e.g.* [28, 29, 30]. In addition to `Isajet7.80` [23], which we use for the spectrum calculation, we use `SuperIso2.7` [31] for computing B-physics observables and `micrOMEGAs2.4` [32] for the calculation of the neutralino LMP abundance.

³With a common value of $m_0(3)$, the $\tilde{\nu}_{\tau}$ LMP may be surprising since at the one-loop level Yukawa interactions drive $m_{\tilde{\tau}_R}^2$ to smaller values than $m_{\tilde{\tau}_L}^2$. In this case, however, two-loop effects due to heavy scalars are large, and for smaller values of $m_{1/2}$ can lead to $m_{\tilde{\tau}_L} < m_{\tilde{\tau}_R}$ and a sneutrino LMP because of the D -term. Since one-loop effects increase with $m_{1/2}$, ultimately the usual situation with stau LMP is obtained. Incidentally, the compensation between the one and two-loop contributions implies that for certain parameters we can have a near equality of the left- and right-stau mass parameters, and so large stau mixing even though the tau Yukawa coupling is not particularly large.

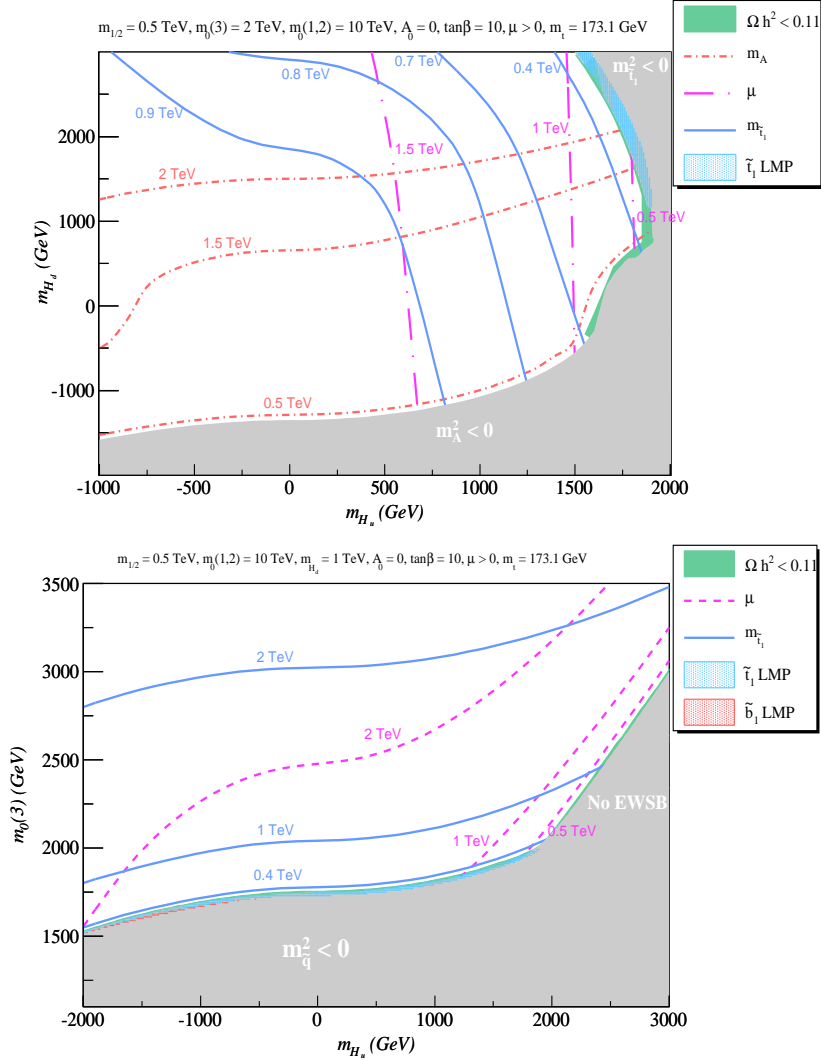


Figure 3: The upper frame a) shows contours of μ , $m_{\tilde{t}_1}$ and m_A in the m_{H_u} vs. m_{H_d} plane for $m_0(1,2) = 10$ TeV, $m_0(3) = 3$ TeV, $m_{1/2} = 0.5$ TeV, $A_0 = 0$, $\tan\beta = 10$ and $\mu > 0$. In the green band, the thermal relic abundance $\Omega_{\tilde{Z}_1} h^2 < 0.11$ and in the shaded blue region the \tilde{t}_1 is the lightest MSSM particle. The gray shaded region is excluded as explained in the text. The lower frame b), shows contours of μ and $m_{\tilde{t}_1}$ in the m_{H_u} vs. $m_0(3)$ plane for $m_0(1,2) = 10$ TeV, $m_{1/2} = 0.5$ TeV, $m_{H_d} = 1$ TeV, $A_0 = 0$, $\tan\beta = 10$ and $\mu > 0$.

For each point P in the scan of ESUSY parameter space, we first compute individual likelihoods $L(O_i)$ for each experimental observable O_i . Then the overall likelihood is given as the product of these individual likelihoods as $L_P = \prod L(O_i)$. The observables we use are listed in Table 1 along with the parameters of the corresponding likelihood functions used. The forms of these likelihood functions are given by,

$$L_1(x, x_0, \sigma_x) = \frac{1}{1 + \exp[-(x - x_0)/\sigma_x]}, \quad L_2(x, x_0, \sigma_x) = \exp\left[-\frac{(x - x_0)^2}{2\sigma_x^2}\right], \quad (3)$$

Observable	Limit	Likelihood function	Ref.
$\text{BF}(b \rightarrow s\gamma)$	$(3.52 \pm 0.34) \times 10^{-4}$	$L_2(x, 3.52 \times 10^{-4}, 0.34 \times 10^{-4})$	[34, 35]
$\text{BF}(B_s \rightarrow \mu^+ \mu^-)$	$\leq 5.8 \times 10^{-8}$	$L_1(x, 5.8 \times 10^{-8}, -5.8 \times 10^{-10})$	[36]
$R(B_u \rightarrow \tau \nu_\tau)$	1.28 ± 0.38	$L_2(x, 1.28, 0.38)$	[34]
m_t	173.1 ± 1.3	$L_2(x, 173.1, 1.3)$	[37]
m_h	≥ 114.5	1 or $\exp(-\chi^2(m_h)/2)$	[33]
SUSY mass limits	LEP limits	1 or 10^{-9}	[38]

Table 1: Observables used in the likelihood calculation.

for observables for which there is only an upper or lower bound, and for observables for which a measurement is available, respectively. For the LEP limit on the Higgs mass, we use [33]

$$\chi^2(m_h) = \frac{(m_h - m_h^{\text{limit}})^2}{(1.1 \text{ GeV})^2 + (1.5 \text{ GeV})^2} \quad (4)$$

with $m_h^{\text{limit}} = 115 \text{ GeV}$. The likelihood $L(m_h)$ is then given by $L(m_h) = e^{-\chi^2(m_h)/2}$ for $m_h < 115 \text{ GeV}$ and $L(m_h) = 1$ for $m_h \geq 115 \text{ GeV}$.

In order to favour (sub)TeV-scale electroweak gauginos, higgsinos, and third generation sfermions, we multiply the likelihood obtained from the experimental constraints with the following model prior:

$$L_{M_{\text{eff}}}(m_X) = \frac{1}{1 + \exp((m_X - M_{\text{eff}})/170 \text{ GeV})} \quad (5)$$

for each $X = \tilde{\chi}_1^+, \tilde{\chi}_2^+, \tilde{t}_1, \tilde{t}_2, \tilde{b}_1$. Choosing, for instance, $M_{\text{eff}} = 1.5 \text{ TeV}$, we get $L_{M_{\text{eff}}} = 0.95, 0.5, 0.05$ for $m_X = 1, 1.5$ and 2 TeV respectively; for $M_{\text{eff}} = 1 \text{ TeV}$, we get $L_{M_{\text{eff}}} = 0.95, 0.5, 0.05$ for $m_X = 0.5, 1, 1.5 \text{ TeV}$ respectively. We have run chains for different M_{eff} and checked that the effect is indeed only to vary the upper bound on the effective SUSY masses; the qualitative features of the parameter space remain unchanged.

Finally, regarding the model parameters, we allow $m_{1/2} = [0, 2] \text{ TeV}$, $m_0(3) = [0, 10] \text{ TeV}$, $m_{H_{u,d}} = [-10, 10] \text{ TeV}$ (with $m_{H_{u,d}}$ unrelated), $A_0 = [-40, 40] \text{ TeV}$, and $\tan \beta = [2, 60]$, taking flat prior probability distributions for all these parameters. In addition we let the top mass vary within $m_t = 173.1 \pm 1.3 \text{ GeV}$ [39] with a Gaussian distribution. For $m_0(1, 2)$, we show results for two different approaches:

1. we let $m_0(1, 2)$ vary from 5 to 20 TeV with a flat prior probability distribution ($L_{\tilde{M}} \equiv 1$),
or
2. we let $m_0(1, 2)$ vary without limits but apply a model prior of

$$L_{\tilde{M}}(m_0(1, 2)) = \frac{1}{1 + \exp((10 - m_0(1, 2))/1.7 \text{ TeV})}, \quad (6)$$

in order to favour $m_0(1, 2)$ values beyond 10 TeV.

The total likelihood of a point is then taken to be $L_{\text{tot}} = L_P \times L_{M_{\text{eff}}} \times L_{\widetilde{M}}$.

Before turning to the results, a comment is in order regarding the nature of the LMP. If we do not impose any dark matter requirement on the LMP, the large majority of points have a neutralino LMP with a far too high relic density of up to $\Omega_\chi h^2 \sim 10^3$. As noted in the Introduction, this can be in agreement with cosmological observations if the “true” LSP is actually an axino, *i.e.* in the case of mixed axion/axino dark matter [12, 40]. Moreover, about 12% (4%) of the points accepted by the chains with $M_{\text{eff}} = 1$ (1.5) TeV have a stop, sbottom or stau LMP. Again these points may be viable if the true LSP is the axino. However, as we will discuss below, the phenomenology in these charged LMP cases is quite different from the neutralino LMP case: in particular, if the stop, sbottom or stau LMP does not decay promptly but gives a charged track. In what follows, we will confine our MCMC analysis to the case of a neutralino LMP, which indeed occurs most frequently. We will, however, comment on the phenomenology of the colored or charged LMP case at the end of the next section.

3.2 MCMC results with neutralino LMP

Figure 4 shows the posterior probability distributions of the input parameters of the ESUSY model from MCMC scans requiring a neutralino LMP. Here we have used $M_{\text{eff}} = 1$ TeV in Eq. (5). Unseen dimensions are marginalized over. The figure compares the two priors for $m_0(1, 2)$: The thin black lines are for case 1. where $m_0(1, 2) = 5\text{--}20$ TeV with a flat distribution, while the thick red lines are for case 2. which has no limits on $m_0(1, 2)$ but the choice of the prior in Eq. (6) favours higher values of $m_0(1, 2)$. We see that, as anticipated, we find solutions where third generation sfermion and gaugino SSB parameters are typically 1–2 TeV, while the first/second generation SSB parameters are favoured to lie beyond 10 TeV. Moderate values of $\tan\beta$ are favoured.

As can be seen, the precise condition on $m_0(1, 2)$ hardly influences the probability distributions of the other parameters. A possible exception is $m_{1/2}$, which features a double-peak distribution. This comes from the fact that at small $m_{1/2}$, the parameter space volume is constrained in the directions of the scalar mass parameters, while there is more space in the $\tan\beta$ direction. For large $m_{1/2}$, on the other hand, $\tan\beta$ is very much constrained by $\text{BR}(b \rightarrow s\gamma)$, while there is more volume in the large $m_0(1, 2)$ directions. The effect is more pronounced for case 1. which does not disfavour smaller values for $m_0(1, 2)$. Moreover, we see that larger $m_0(1, 2)$ prefers somewhat larger $m_{1/2}$.⁴ It is also interesting to note that very high $m_0(1, 2)$ around 15–20 TeV suffers from a low probability. This is because as $m_0(1, 2)$ increases, we are forced to increasing larger values of $m_0(3)$ (see Fig. 1). For values of $m_0(3)$ in the multi-TeV range, third generation SSB parameters at \lesssim TeV can occur only when the large two loop RGE contributions rather precisely cancel the naturally multi-TeV contribution that we start with – too little cancellations leave large SSB parameters, while too much cancellation leads to tachyonic masses. As a result, the region of parameter space with a light third generation rapidly shrinks when $m_0(1, 2)$ exceeds $\sim 15\text{--}20$ TeV.

⁴The shape of the posterior probability distribution of $m_{1/2}$, and $\tan\beta$ are likely the most sensitive to the $b \rightarrow s\gamma$ constraint, and hence to our assumption that there are no off-diagonal pieces in the GUT scale squark mass matrices.

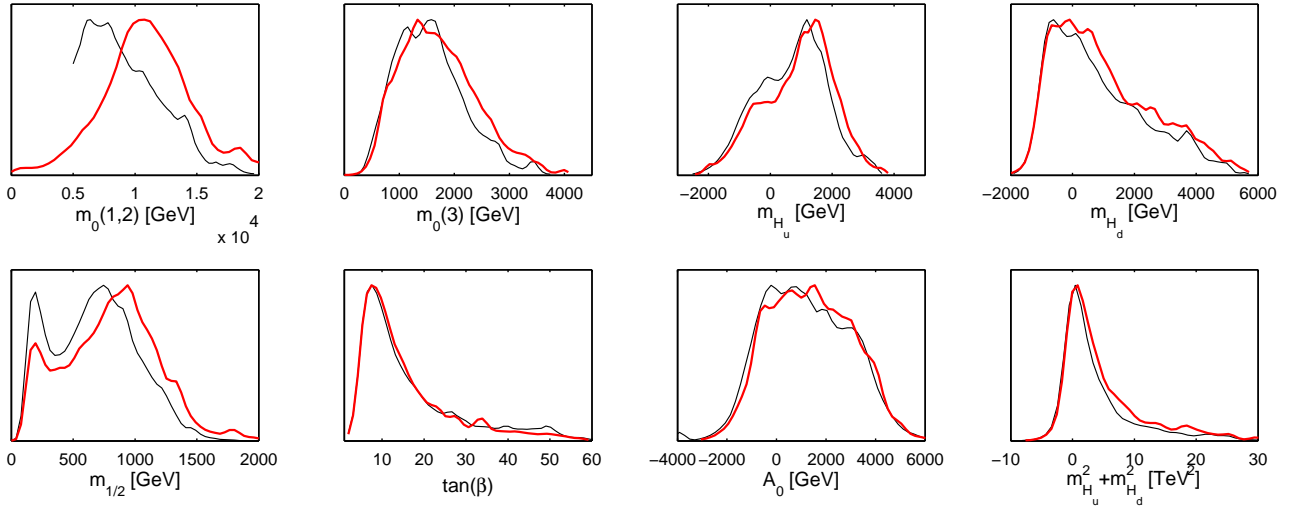


Figure 4: Posterior probability distributions of the input parameters of the ESUSY model from MCMC scans with $M_{\text{eff}} = 1$ TeV, comparing the two priors for $m_0(1, 2)$. We take $\mu > 0$, and assume that the neutralino is the LMP. The thin black lines are for case 1. where $m_0(1, 2) = 5 - 20$ TeV with a flat distribution, while the thick red lines are for case 2. which has no limit on $m_0(1, 2)$ but the prior Eq. (6) disfavors low values for this parameter. The last panel shows the combination $m_{H_u}^2 + m_{H_d}^2$.

The posterior probability distributions of several relevant masses are shown in Fig. 5. We infer from the EW gaugino spectrum (and also the μ) distribution that most of the time the lightest neutralino is bino-like.

Figure 6 displays the probability distributions of B -decay observables, $\Delta a_\mu = (g - 2)_\mu^{\text{SUSY}}$, the higgsino fraction $f_H = v_1^{(1)2} + v_2^{(1)2}$ (in the notation of Ref. [22]) of the \tilde{Z}_1 , and the relic abundance Ωh^2 of the \tilde{Z}_1 . It is clear that if the muon anomalous moment is confirmed, it cannot arise within the ESUSY framework. We note that there is non-negligible fraction of the parameter space with a higgsino-like LMP. We also see that the neutralino relic density peaks around $\Omega h^2 \simeq 1 - 10$ and goes up to $\Omega h^2 \sim 10^4$. Nevertheless, solutions with low values of $\Omega h^2 \lesssim 0.1$, where the relic density of thermal neutralinos does not yield a universe that is too short-lived, also have non-negligible probability. They occur because of Higgs funnel annihilation, coannihilation with light stops and/or sbottoms (or, less likely, staus), or because of a large LMP higgsino component.

3.3 Effective SUSY benchmark points

To illustrate the types of SUSY spectra and the diverse phenomenology that can result in ESUSY models, we list five benchmark points in Table 2. The first three points we list have a neutralino LMP, while points ES4 and ES5 have a sbottom and a stau LMP, respectively. Point ES1 adopts an $m_0(1, 2) = 10$ TeV, which is the most favored value in the probability distributions resulting from the MCMC. On the other hand, ES1 has a value of $m_{\tilde{g}} = 524$ GeV, not far from the ESUSY minimum of $m_{\tilde{g}} \gtrsim 460$ GeV. The chargino \tilde{W}_1 and the neutralino \tilde{Z}_2

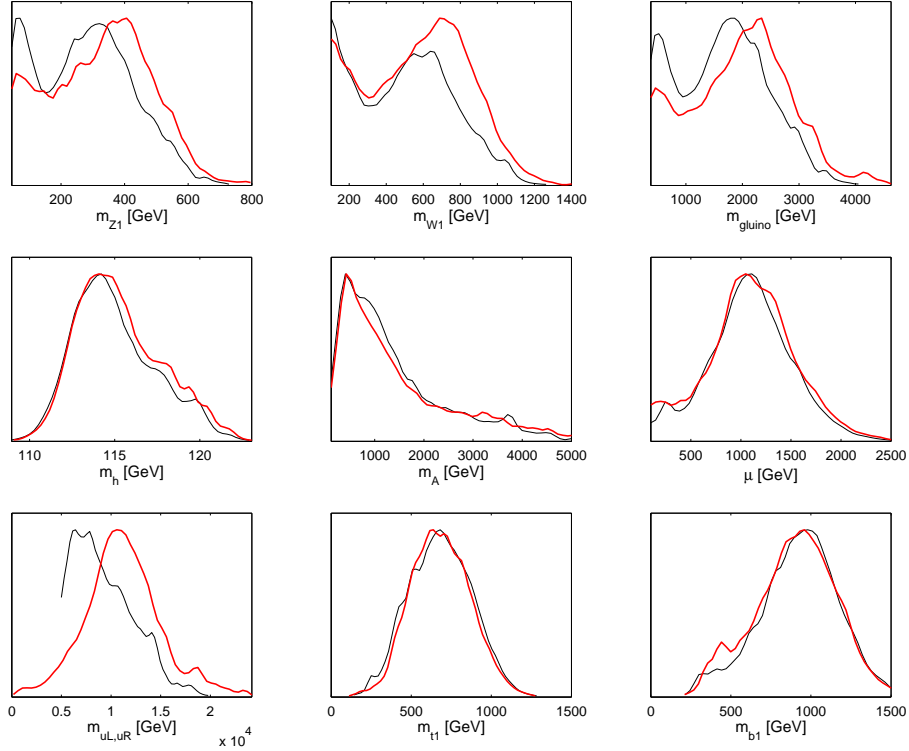


Figure 5: Same as Fig. 4 but for various sparticle and Higgs masses, and μ .

have masses of just 139 GeV, and the μ parameter is 857 GeV. All third generation squarks except \tilde{b}_2 , as well as all EW gauginos are ~ 1 TeV scale, while the two staus are over 2 TeV.

In point ES2, $m_0(1, 2)$ is increased to 12 TeV. ES2 has much higher value of $m_{\tilde{g}} \sim 2.4$ TeV with concomitantly heavier \tilde{W}_1 and $\tilde{Z}_{1,2}$, although all EW gauginos along with \tilde{t}_1 , \tilde{t}_2 and \tilde{b}_1 are below 1 TeV. The \tilde{b}_2 and staus all have masses $\sim 1.3 - 1.4$ TeV range. For this point, \tilde{t}_1 decays exclusively via the three-body mode $\tilde{t}_1 \rightarrow bW\tilde{Z}_1$, while other third generation quarks decay via two-body decays.

Point ES3, with a value of $m_0(1, 2) \simeq 10$ TeV, again has all third generation sfermions, as well as all charginos, neutralinos and Higgs bosons essentially at or well below 1 TeV. The gluino mass is rather high: ~ 2.1 TeV. One characteristic feature of this point is that, because of the near degeneracy of \tilde{t}_1 and \tilde{Z}_1 , not only the two-body decays but even the three body decay $\tilde{t}_1 \rightarrow bW\tilde{Z}_1$ is kinematically forbidden. In this case, \tilde{t}_1 will decay via $\tilde{t}_1 \rightarrow c\tilde{Z}_1$ or $\tilde{t}_1 \rightarrow b\tilde{Z}_1 f\bar{f}'$, though of course the small available phase space will favour the former decay [41].

Point ES4 has a high $m_0(1, 2) = 20$ TeV, a heavy gluino with a mass of 2.5 TeV, and correspondingly heavy EW gauginos. However, \tilde{t}_1 and \tilde{b}_1 are very light with masses of 327 GeV and 291 GeV, while $m(\tilde{t}_2) = 793$ GeV. In this case, \tilde{b}_1 is the LMP.

Finally, point ES5 has been chosen to illustrate that staus can also be very light. Here, $\tilde{\tau}_1$ is the LMP, with a mass of just 289 GeV, while $m(\tilde{\tau}_2) = 380$ GeV. The lighter stop and the EW gauginos are in the sub-TeV range, while other third generation sfermions are 1.1-1.2 TeV.

Two of the ESUSY points with a neutralino as LMP (ES1 and ES2) yield a thermal abundance of neutralinos far in excess of WMAP measured value for the cold DM relic density, while

parameter	ES1	ES2	ES3	ES4	ES5
$m_0(1, 2)$ [TeV]	10	12	10	20	6
$m_0(3)$ [TeV]	2.4	1.5	1.1	3.3	0.3
m_{H_d} [TeV]	1	-0.35	-0.6	1	0
m_{H_u} [TeV]	2	1.2	0.5	1	0
$m_{1/2}$ [TeV]	0.16	1	0.85	1	0.8
A_0 [TeV]	0	0.9	1	0	0
μ	857	902	925	2329	855
$m_{\tilde{g}}$	524	2446	2103	2526	1941
$m_{\tilde{u}_L}$ [TeV]	10.0	12.1	10.1	20.1	6.2
$m_{\tilde{u}_R}$ [TeV]	10.0	12.2	10.1	20.1	6.2
$m_{\tilde{e}_L}$ [TeV]	10.0	12.0	10.0	20.0	6.0
$m_{\tilde{e}_R}$ [TeV]	10.0	12.0	10.0	20.0	6.0
$m_{\tilde{t}_1}$	646	608	398	327	867
$m_{\tilde{t}_2}$	1049	948	770	793	1147
$m_{\tilde{b}_1}$	1039	830	586	292	1083
$m_{\tilde{b}_2}$	1711	1313	958	1885	1176.3
$m_{\tilde{\tau}_1}$	2269	1341	944	2956	289
$m_{\tilde{\tau}_2}$	2299	1388	1008	3152	381
$m_{\tilde{W}_1}$	139	815	708	881	658
$m_{\tilde{Z}_2}$	139	815	708	878	657
$m_{\tilde{Z}_1}$	69	441	372	452	347
m_A	1022	450	398	2042	875
m_h	110.7	118.3	117.3	119.9	117.8
$\Omega_{\tilde{Z}_1} h^2$	320	0.789	0.036	-	-
σ [fb]	23.2×10^3	157.8	1618.0	12.3×10^3	51.4
$\tilde{g}\tilde{g}$	62.8%	0.02%	0.01%	-	1.5%
<i>EW - ino pairs</i>	36.6%	5.1%	0.8%	0.06%	35.3%
<i>slep. pairs</i>	-	0.02%	0.01%	-	24.4%
$\tilde{t}_1\tilde{t}_1$	0.4%	78.3%	87.6%	28.2%	26.5%
$\tilde{t}_2\tilde{t}_2$	0.03%	4.5%	1.8%	0.3%	3.8%
$\tilde{b}_1\tilde{b}_1$	0.02%	11.5%	9.1%	71.4%	4.9%
$\tilde{b}_2\tilde{b}_2$	-	0.4%	0.4%	-	2.9%

Table 2: Masses and parameters in GeV units (unless otherwise noted) for five case study points in ESUSY using Isajet 7.80 with $m_t = 173.1$ GeV, $\tan\beta = 10$ and $\mu > 0$. The LMP mass is denoted with bold numbers. We also list the total tree level sparticle production cross section in fb at the LHC with a center of mass energy of 14 TeV.

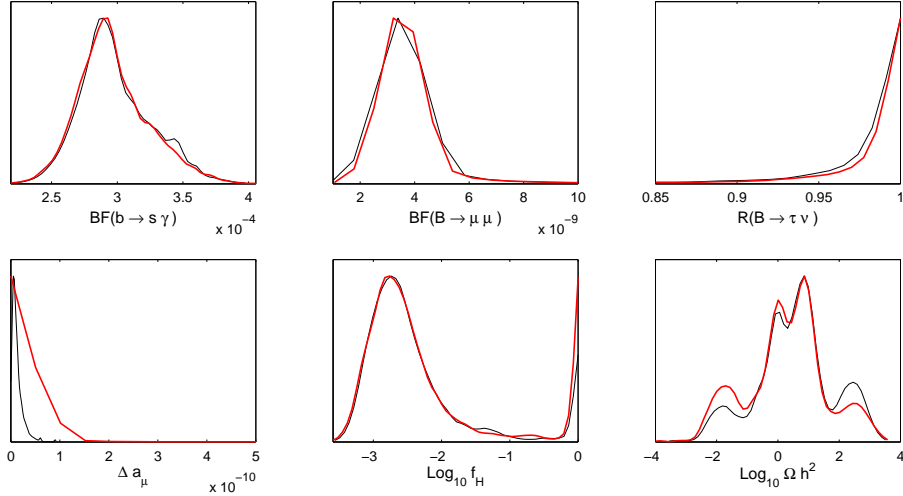


Figure 6: *Same as Fig. 4 but for a variety of low energy observables, the higgsino content of the lightest neutralino, and the thermal neutralino relic density.*

point ES3 is in the top-squark co-annihilation region and gives a thermal neutralino abundance of $\Omega_{\tilde{Z}_1} h^2 = 0.036$. As mentioned previously, the points ES1 and ES2 can still be cosmologically viable if we invoke the PQWW solution to the strong CP problem, which necessitates the introduction of an axion/axino supermultiplet into the theory. In this case, the axino \tilde{a} , and not the neutralino, can be the LSP. If the \tilde{a} is the LSP, then the neutralinos will decay via $\tilde{Z}_1 \rightarrow \tilde{a}\gamma$ with lifetime smaller than $\lesssim 0.1\text{--}1\text{ s}$, *i.e.* before the onset of Big Bang nucleosynthesis (BBN), for a PQWW scale $f_a \lesssim 10^{12}$ GeV [42]. Since every neutralino decays to an axino, the would be thermal relic density of neutralinos is reduced by a factor $m_{\tilde{a}}/m_{\tilde{Z}_1}$, and for small enough $m_{\tilde{a}}$ would be compatible with the relic density measurement. Thermal production of axinos in the early universe can still proceed, but the relic abundance of axinos then depends on the re-heat temperature T_R after inflation. The dark matter will then consist of an axino/axion admixture [12], with relic axions being produced via the vacuum mis-alignment mechanism.

In the cases where \tilde{t}_1 , \tilde{b}_1 or $\tilde{\tau}_1$ are LMPs, such scenarios are again allowed if, as before, we assume that the axino is the LSP. In these cases the sfermions dominant decay is $\tilde{f}_1 \rightarrow f\tilde{a}$, via loop-mediated processes; the competing three-body decays, $\tilde{\tau}_1 \rightarrow \tau\tilde{a}\gamma$ [43] or $\tilde{q} \rightarrow q\tilde{a}g$ [44] are argued to have a small branching fraction. The loop calculation is complicated by the fact that the non-renormalizable axino-bino-photon (and the axino-bino-Z and axino-gluino-gluon) coupling enters the calculation. Nevertheless, these authors find that for $m_{\tilde{\tau}} = 100$ GeV, the stau LMP lifetime ranges from about 0.01 s to 10 h, for the PQWW scale f_a in the range $5 \times 10^9 - 5 \times 10^{12}$ GeV, and scales inversely as the stau mass. The corresponding squark lifetime is shorter: about 2×10^{-6} s for 500 GeV squarks and 1 TeV gluinos with $f_a = 10^{11}$ GeV. If the LMP lifetime indeed exceeds a few seconds, this could disrupt the successful predictions of Big Bang nucleosynthesis [45], though it appears that if $f_a < 10^{12}$ GeV, a stau LMP is relatively safe [46]. For a general discussion of charged LMPs, see Ref. [47].

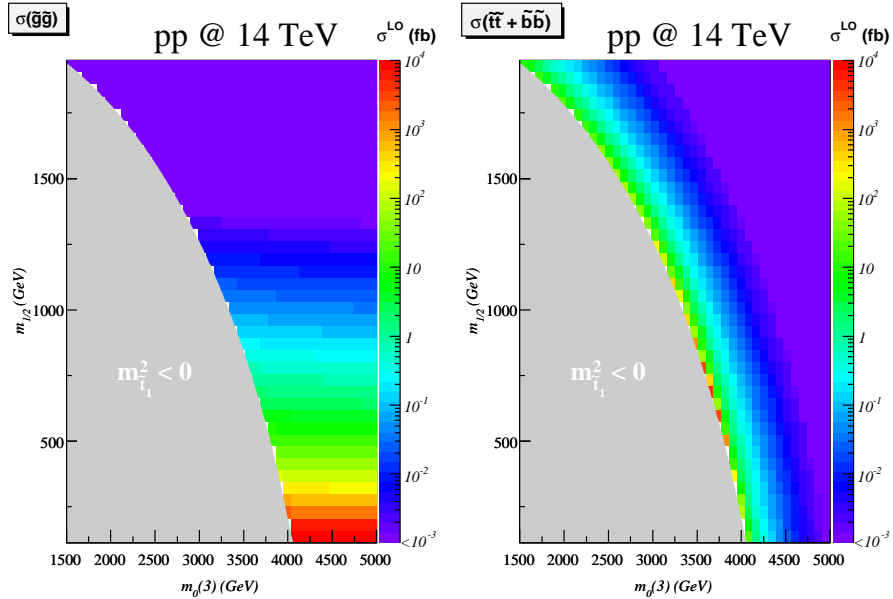


Figure 7: a) Gluino pair production and b) third generation squark pair production cross sections at LHC with $\sqrt{s} = 14$ TeV in the $m_0(3)$ vs. $m_{1/2}$ plane for $m_0(1,2) = 20$ TeV, $m_{H_{u,d}} = 1$ TeV and $A_0 = 0$, $\tan\beta = 10$ and $\mu > 0$.

4 Phenomenology of Effective SUSY at the LHC

How will effective SUSY manifest itself at the LHC? To answer this, we first show in Fig. 7 total gluino and third generation squark pair production cross sections at a 14 TeV pp collider in the $m_0(3)$ vs. $m_{1/2}$ plane displayed in Fig. 2, but now with $m_0(1,2) = 20$ TeV. In frame a), the $pp \rightarrow \tilde{g}\tilde{g}X$ reaction (where X denotes assorted hadronic debris) reaches to over 10^4 fb for gluino masses as low as $m_{\tilde{g}} \lesssim 500$ GeV. The gluino pair cross section drops continuously as $m_{1/2}$, or alternatively $m_{\tilde{g}}$, increases.

The ESUSY region with third generation squarks having masses \lesssim TeV lies adjacent to the boundary of the gray tachyonic region. In frame b), we see the $pp \rightarrow \tilde{t}_i\tilde{t}_i$ plus $\tilde{b}_i\tilde{b}_i$ (for $i = 1 - 2$) summed cross sections. These are typically in the 1-100 fb range all along the tachyonic boundary, with portions reaching cross sections as high as 10^3 fb. Thus, the low $m_{1/2}$ region will consist of mainly gluino pair production, where the main influence of light third generation squarks will be upon the gluino branching fractions. As we move to higher $m_{1/2}$ values, the gluino pair cross section will diminish, and the total SUSY production cross section will be dominated by pair production of third generation squarks.

Unless the gluino is very heavy we would expect that, especially after selection cuts, LHC phenomenology would largely be determined by gluino pair production. SUSY event topologies would thus be sensitive to gluino decay patterns. In Fig. 8, we show the gluino branching fractions for the MCMC scan points with $m_{\tilde{g}} \leq 1$ TeV. Of course, when gluino two-body decays are kinematically accessible, these would dominate. We see from the figure that these are accessible for relatively few points when $m_{\tilde{g}} < 500$ GeV. We will return to this later when

we discuss how one might distinguish the ESUSY model with light gluinos from the model with t - b - τ Yukawa unification where $m_{\tilde{g}}$ is bounded from above [17]. For the bulk of the scanned points, the gluino decays via three body modes into top and bottom quarks plus EW gauginos; corresponding decays to the first two generations are suppressed because these squarks are very heavy. Bottom-jet tagging will clearly provide an effective way for enriching the ESUSY event sample at the LHC [48, 49]. As in many SUSY models, direct decays to the neutralino LMP never have a very large branching fraction. The fact that gluino decays have large branching fractions to \widetilde{W}_1 , \widetilde{Z}_2 and top quarks implies that the ESUSY gluino event sample will include multi-lepton events from gluino decay cascades. Finally, we see from the last frame that while the branching fraction for the radiative gluino decays [50] $\tilde{g} \rightarrow g\widetilde{Z}_i$ is usually small, it can reach 40–50%. We have checked that the neutralino in question is mostly $\widetilde{Z}_{3,4}$. This occurs when we have large splittings among third generation squarks with stops being lighter than sbottoms, when a light neutralino has a significant up-higgsino component and the decay $\tilde{g} \rightarrow t\bar{t}\widetilde{Z}_1$ is kinematically forbidden. The branching fraction for decays to light quarks is very small for $m_0(1, 2) > 5$ TeV, although larger values are possible with the second $L_{\widetilde{M}}$ prior (case 2. in Sec. 3.1), which disfavors lower values of $m_0(1, 2)$ but does not exclude them.

4.1 Light gluinos with \widetilde{Z}_1 as LMP (ES1)

The benchmark point ES1 features a rather light gluino with mass $m_{\tilde{g}} = 524$ GeV, correspondingly light charginos and neutralinos, along with three sub-TeV third generation squarks. From Table 2, we see that total sparticle production cross section, summed over all reactions, is 23.2 pb. Of this, 62.8% comes from $pp \rightarrow \tilde{g}\tilde{g}X$ production, while 36.6% comes from EW gaugino production (sum of all chargino and neutralino production cross sections). Only a tiny fraction of the production cross section comes from third generation squarks, so the rate for $\tilde{t}_i\tilde{t}_i$ and $\tilde{b}_i\tilde{b}_i$ production (for $i = 1, 2$) is very small.

The gluino decays via three body modes as $\tilde{g} \rightarrow b\bar{b}\widetilde{Z}_2$ (37%), $\tilde{g} \rightarrow t\bar{t}\widetilde{Z}_1$ (19%) and $\tilde{g} \rightarrow t\bar{b}\widetilde{W}_1 + c.c$ (41%). Thus, each gluino pair production event will contain at least four b -jets, plus other jets, isolated leptons (from top quarks and EW gauginos) and E_T^{miss} . The \widetilde{W}_1 decays via three-body modes $\widetilde{W}_1 \rightarrow \widetilde{Z}_1 f \bar{f}'$ in accord with W^* propagator dominance (*e.g.* $\widetilde{W}_1 \rightarrow \widetilde{Z}_1 e \bar{\nu}_e$ at 11%). The \widetilde{Z}_2 decays to $b\bar{b}\widetilde{Z}_1$ 20% of the time, while leptonic decays such as $\widetilde{Z}_2 \rightarrow \widetilde{Z}_1 e^+ e^-$ occur at the 3% level. In this case, the \tilde{b}_1 is quite light and dominantly \tilde{b}_L , which enhances the \widetilde{Z}_2 decay to b quarks at the expense of first and second generation fermions. Clean tripleton signals from $\widetilde{W}_1\widetilde{Z}_2$ production may also be observable [51].

The ES1 scenario will have much the same LHC phenomenology as the Yukawa-unified SUSY with a 500 GeV gluino [49], which is also dominated by gluino pair production followed by three-body gluino decays into mainly b -quarks. A natural question to ask is whether it is possible to distinguish these scenarios at the LHC. One difference is that Yukawa-unified SUSY requires a very large A_0 parameter with $A_0 \sim -2m_{16}$, where m_{16} is the matter GUT scale scalar mass parameter, which lies typically in the range 8–20 TeV. This large value of A_0 feeds into gaugino mass evolution at two-loops in the RGEs, and suppresses $m_{\tilde{g}}$ with respect to $m_{\widetilde{Z}_1}$ and $m_{\widetilde{Z}_2, \widetilde{W}_1}$.

To illustrate this, we show in Fig. 9 a scatter plot of $m_{\tilde{g}}$ versus $m_{\widetilde{Z}_2} - m_{\widetilde{Z}_1}$ obtained by

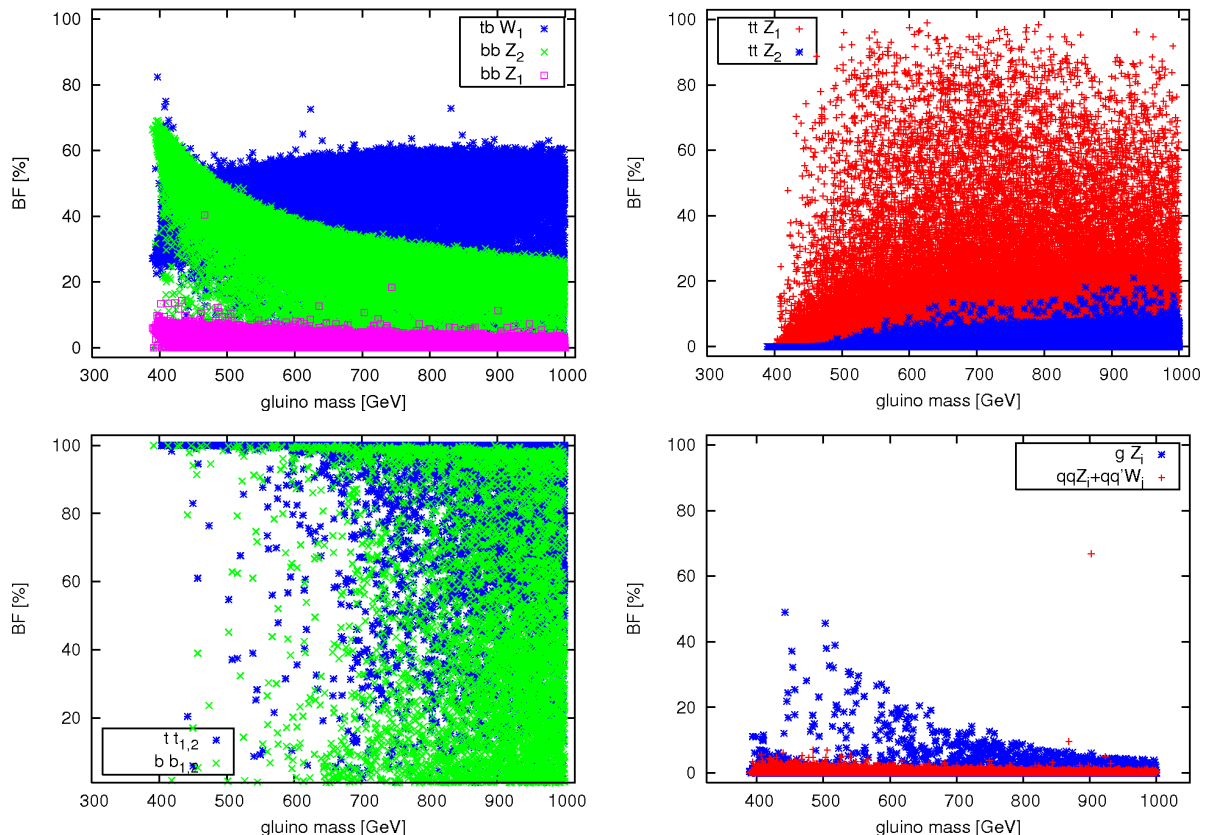


Figure 8: Results for the branching fractions for gluino decays from MCMC scan points with $m_{\tilde{g}} \leq 1$ TeV versus the gluino mass. The upper two frames show the branching fractions for three-body decays of gluinos to third generation quarks plus EW gauginos. The bottom-left frame shows the branching fraction for two-body decays to third generation quarks and squarks, while the bottom-right frame illustrates that the radiative decays $\tilde{g} \rightarrow g\tilde{Z}_i$ can sometimes be substantial. All results are for the $L_{\tilde{M}} = 1$ case with $5 \text{ TeV} < m_0(1, 2) < 20 \text{ TeV}$.

scanning the parameter space of (a) the ESUSY model (red pluses) and (b) the Yukawa-unified (YU) model with “just-so” GUT scale Higgs soft mass splitting (HS, dark blue stars) and the YU model with full D -term splitting, right-hand neutrinos and 3rd generation scalar splitting (the DR3 model [52], light blue squares). Here, we require in YU models that R , the ratio of the largest to the smallest of the GUT scale Yukawa couplings, is smaller than 1.05. While there is significant overlap of the two classes of Yukawa-unified models, the ESUSY model lies on a distinct band. We expect that the neutralino mass difference edge will be rather well determined by the $m(\ell^+\ell^-)$ distribution. Then, even a crude measure of the gluino mass at the 10–20% level via M_{eff} [53] or total cross section [54] would suffice for this distinction. Also, in Ref. [49], it is shown that the mass difference $m_{\tilde{g}} - m_{\tilde{Z}_2}$ might be extracted via the kinematic edge in the $m(bb)$ distribution.⁵ If $m_{\tilde{g}}$ can be determined even more precisely using m_{T2} [55],

⁵ We have also checked that a scatter plot of $m_{\tilde{g}} - m_{\tilde{Z}_2}$ vs. $m_{\tilde{Z}_2} - m_{\tilde{Z}_1}$ also serves to separate the ESUSY model from the Yukawa-unified SUSY scenarios, but do not show it here for brevity.

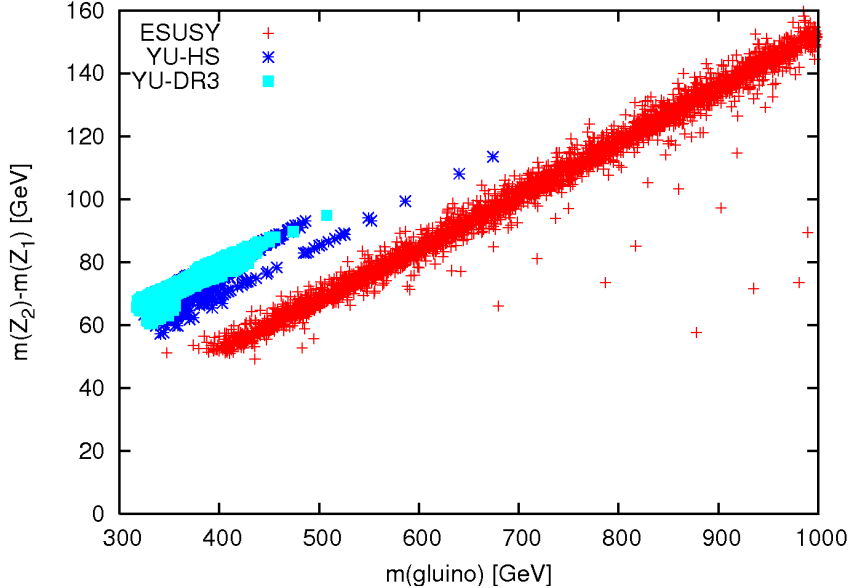


Figure 9: Scatter plot of the gluino mass versus the neutralino mass difference $m_{\tilde{Z}_2} - m_{\tilde{Z}_1}$ that can be obtained from the determination of the dilepton mass edge at the LHC. We show results for the ESUSY model (red), and two different models with t - b - τ Yukawa unification (medium and light blue) discussed in the text.

its generalizations [56], or other methods that have recently been suggested, the distinction between the models would be even sharper.

4.2 Light top and bottom squarks, heavy gluinos and \tilde{Z}_1 as LMP (ES2 & ES3)

For point ES2, since $m_{1/2}$ is large, the value of $m_{\tilde{g}}$ is also large, and so $\tilde{g}\tilde{g}$ will not be produced at an appreciable rate at LHC. Instead, the total SUSY cross section of $\sigma_{SUSY} = 157.8$ fb is dominated by 78.3% $\tilde{t}_1\tilde{t}_1$ production, and 11.5% $\tilde{b}_1\tilde{b}_1$ production. A few percent of $\tilde{t}_2\tilde{t}_2$ also contribute. The $\tilde{t}_1 \rightarrow bW\tilde{Z}_1$ decay occurs at nearly 100% branching fraction, so the $\tilde{t}_1\tilde{t}_1$ production results in a $b\bar{b}W^+W^- + E_T^{\text{miss}}$ final state. This should be separable from $t\bar{t}$ background if large E_T^{miss} or M_{eff} is required. Another possible background is $Zt\bar{t}$ production. Because gluinos are heavy, SUSY contamination to the signal [57] is not an issue. The $\tilde{b}_1 \rightarrow W\tilde{t}_1$ decays at nearly 100% branching fraction, so this component of the production cross section will result in a $b\bar{b}W^+W^-W^+W^- + E_T^{\text{miss}}$ final state.

The case of ES3 has four sub-TeV third generation squarks plus tau-sleptons near a TeV or below. The total production cross section of $\sigma_{SUSY} = 1618$ fb comes from 87.6% $\tilde{t}_1\tilde{t}_1$ production, 9.1% $\tilde{b}_1\tilde{b}_1$ production plus a few percent of heavier top and bottom squark pairs. The visible decay products from \tilde{t}_1 decay will be soft since there is only a 26 GeV mass gap between the \tilde{t}_1 and the \tilde{Z}_1 ; the visible decay products of \tilde{t}_1 may not reliably detectable unless they are boosted. The $\tilde{b}_1 \rightarrow W\tilde{t}_1$ at nearly 100% branching fraction, so from $\tilde{b}_1\tilde{b}_1$ production we expect a $W^+W^- + E_T^{\text{miss}}$ final state, accompanied by soft charm jets or other soft hadronic

debris. The possible background comes from W^+W^-Z production.

Before turning to the next benchmark case we remark that, although we have not examined an example of such a benchmark point, it has been shown [58] that if the gluinos and stops both have sub-TeV masses and that the decays $\tilde{g} \rightarrow t\tilde{t}_1 \rightarrow tb\tilde{W}_1$ and/or $\tilde{g} \rightarrow b\tilde{b}_1 \rightarrow bt\tilde{W}_1$ are kinematically accessible and occur with large branching fractions, a partial reconstruction of the event using techniques to tag the secondary top quark may be possible. Moreover, in [59] it has been shown that if $\tilde{g} \rightarrow t\tilde{t}_1 \rightarrow tc\tilde{Z}_1$ dominates, the signature of 2 b-jets plus 2 same-sign leptons plus additional jets and missing energy is an excellent discovery channel for gluino masses up to about 900 GeV.

4.3 Bottom or top squarks as LMP: the case of heavy quasi-stable colored particles (ES4)

Benchmark point ES4 illustrates an ESUSY model with \tilde{t}_1 and \tilde{b}_1 lighter than \tilde{Z}_1 , and in fact the bottom squark \tilde{b}_1 is the LMP. This is viable if the axino is the true LSP so that $\tilde{b}_1 \rightarrow b\tilde{a}$, and the dark matter consists of an axion/axino admixture. For case ES4, with a PQ breaking scale of order $f_a \sim 10^{11}$ GeV, we find a bottom squark lifetime of $\sim 10^{-6}$ sec, *i.e.* the \tilde{b}_1 is stable as far as collider searches go, but it decays well before the start of Big Bang nucleosynthesis. Previous searches for quasi-stable squark hadrons Q at ALEPH find that $m_Q > 95$ (92) GeV for up-type (down-type) squark hadrons [60]. Searches by CDF evidently require $m_Q \gtrsim 241.5$ GeV [61, 62]. At the LHC, for case ES4, sparticles will be produced with total cross section $\sigma_{SUSY} \simeq 1.2 \times 10^4$ fb, of which 71.4% is $\tilde{b}_1\tilde{b}_1$ production, and 28.2% is $\tilde{t}_1\tilde{t}_1$ production. The $\tilde{t}_1 \rightarrow \tilde{b}_1W$ branching fraction is essentially 100%, and so augments the \tilde{b}_1 production rates. The \tilde{b}_1 is a quasi-stable colored particle, and will hadronize to form an R -meson or baryon $B^{\pm,0} = \tilde{b}_1\bar{q}$ or \tilde{b}_1qq' , where q is usually u or d . The properties of squark hadrons have been reviewed in [63, 62]. The heavy B hadron will be produced and propagate through the detector with minimal energy loss due to hadronic interactions. It can be of charge ± 1 or 0, and in fact as it propagates, it has charge exchange reactions with nuclei in the detector material, so that the path of the B -hadron can thus be intermittently charged or neutral [64, 65].

Stable squark hadrons can be detected as muon-like events, albeit with the possibility of intermittently appearing and disappearing tracks. Detection can be made using dE/dx measurements in the tracking system, or time-of-flight (ToF) measurements in the muon system. Measuring both the B hadron momentum and velocity should allow a B mass measurement to about 1-2 GeV [62]. The reach of LHC for quasi-stable squark hadrons has been estimated in Ref. [62]. Using those results, we estimate the LHC reach with $\sqrt{s} = 7$ TeV and 1 fb^{-1} of integrated luminosity to be up to $m_{\tilde{b}_1} \sim 315$ GeV, which would already test point ES4! The LHC reach with $\sqrt{s} = 14$ TeV and 100 fb^{-1} is estimated as $m_{\tilde{b}_1} \sim 800$ GeV, from just $\tilde{b}_1\tilde{b}_1$ production alone. Additional contributions to \tilde{b}_1 production from cascade decays would increase the reach, and also make clear that \tilde{b}_1 -pair production is not the only new physics process occurring at the LHC.

We note also that many cases with a \tilde{t}_1 LMP can also be generated in ESUSY. In these cases, with a quasi-stable top-squark hadron, the lifetime and reach discussion is qualitatively similar to that given above.

4.4 Staus as LMP: the case of heavy quasi-stable charged particles (ES5)

For ESUSY benchmark point ES5, we have $\tilde{\tau}_1$ as LMP. As with point ES4, we may again invoke a lighter axino to escape constraints on charged stable exotics and also mixed axion/axino CDM. In this case, the stau decays through loop diagrams via $\tilde{\tau}_1 \rightarrow \tau\tilde{a}$ with a lifetime typically of order 1 sec for $f_a \sim 10^{11}$ GeV, and does not significantly disrupt BBN [46]. Searches for quasi-stable charged particles at OPAL require $m_{\tilde{\tau}_1} \gtrsim 98.5$ GeV [66].

The quasi-stable stau will propagate slowly through LHC detectors much like a heavy muon, and leave a highly-ionizing track [64]. The dE/dx , ToF and track bending measurements should allow for momentum and velocity, and hence mass determinations.

For case ES5, the total SUSY production cross section is $\sigma_{SUSY} \simeq 51.4$ fb. Of this, just about a quarter comes from stau pair production. However, since all produced sparticles now cascade down into the stau LMP, the total $\tilde{\tau}_1$ production is augmented, in this case, by a factor four. For instance, $\tilde{t}_1\tilde{t}_1$ is produced at 26.5% rate, and $\tilde{t}_1 \rightarrow \tilde{Z}_1 t$ at 53.3%, $\tilde{t}_1 \rightarrow t\tilde{Z}_2$ at 7.4% and $\tilde{t}_1 \rightarrow b\tilde{W}_1$ at 39.3%. Then, $\tilde{Z}_1 \rightarrow \tau^\pm\tilde{\tau}_1^\mp$ at 100% branching fraction. Also, $\tilde{W}_1 \rightarrow \tilde{\tau}_1\nu_\tau$ at 100%, and $\tilde{Z}_2 \rightarrow \tau^\pm\tilde{\tau}_2^\mp$ at 42% and $\tilde{\nu}_\tau\tilde{\nu}_\tau + c.c$ at 49%, while $\tilde{\nu}_\tau \rightarrow \tilde{Z}_1\nu_\tau$, followed by further \tilde{Z}_1 decay. Thus, we expect the cascade decay events to each contain at least two $\tilde{\tau}_1$ tracks, frequently in company of an assortment of τ -jets, together with b quarks and leptons from W -bosons. If the energy of the LMP (as measured from the velocity and momentum of the track) can be included, E_T^{miss} in such SUSY events arises only from neutrinos, and so is not especially large.

The LHC reach for quasi-stable staus has been estimated in [62] in the case where only stau pair production contributes. The reach for LHC at $\sqrt{s} = 14$ TeV with 100 fb^{-1} of integrated luminosity is found to be $m_{\tilde{\tau}_1} \sim 250$ GeV. This is conservative for the present case, since $\tilde{\tau}_1$ production will be augmented by a factor of four from production via cascade decays of heavier sparticles. Moreover, as in the ES4 case, detection of more complicated events other than just stau pair production will bring home the richness of the new physics being detected.

5 Summary and Conclusions

Effective SUSY has been suggested as a model for ameliorating the flavour and CP problems that are endemic to generic SUSY models, while maintaining naturalness in the EWSB sector. The general idea is that SUSY states that have large couplings to the Higgs sector — third generation sfermions and EW gauginos — have masses at or below the TeV scale, while first and second generation sparticles that directly affect the most stringently constrained flavour-changing processes are heavy. The typical ESUSY spectrum consists of multi-TeV first and second generation sfermions along with EW gauginos, Higgs bosons and third generation sfermions at or below the TeV scale; gluinos may be as light as 450 GeV or as heavy as several TeV.

In this paper, we have examined the LHC phenomenology of ESUSY models. Toward this end, we set up the ESUSY model with parameters defined at the GUT scale in Sec. 1. For simplicity of incorporating flavour constraints without greatly impacting LHC physics, we have assumed GUT scale degeneracy of the SSB mass parameters of the first two generations,

but allowed the corresponding parameters for the third generation and Higgs scalars to be independent.

We have delineated the viable parameter space in Sec. 2. In Sec. 3.1, we have described the MCMC setup that was used for finding the portion of the entire parameter space consistent with various low energy constraints as well as lower limits on sparticle and Higgs boson masses along with theory priors that were used to obtain ESUSY spectra. Our results for the favoured ranges of the input parameters, assuming that the LMP is a neutralino (this is true for the bulk of the points), are shown by the posterior probability distributions in Fig. 4. The corresponding distributions for sparticle masses, illustrated in Fig. 5, indeed show the expected qualitative features of the ESUSY spectrum: \lesssim TeV third generation and EW gaugino masses, 10-20 TeV first/second generation squarks (and sleptons, that we did not show), and gluinos ranging from 0.5-4 TeV. The posterior probability distributions for various low energy observables and the thermal neutralino relic density are shown in Fig. 6. While the former generally lie close to their SM values (because of the nature of the ESUSY spectra), the neutralino relic density Ωh^2 ranges from below 0.01 to 10^3 with a peak value around 1 – 10.

We note that models with large values of $\Omega_{\tilde{Z}_1} h^2$ are phenomenologically every bit as viable as models with a thermal neutralino LSP provided the LMP neutralino is not the true LSP, but decays into the LSP before the advent of Big Bang nucleosynthesis. The axino of the axion-axino multiplet which is present in SUSY models with the PQWW solution to the strong CP problem is an excellent example of an LSP that is not the LMP, and indeed models where the measured CDM is comprised of axions and axinos have been studied in the literature. Moreover, if the axino is the LSP, models where the LMP is charged or coloured are also allowed provided again that the LMP decays before nucleosynthesis.

Our main results on the LHC phenomenology of ESUSY models were presented in Sec. 4. The most important sparticle production mechanisms at the LHC are gluino pair production for values of $m_{1/2} \lesssim 700$ GeV, and third generation squark pair production. A very high b -jet multiplicity is the hallmark of multi-jet+multilepton+ E_T^{miss} events within the ESUSY framework. Gluinos mostly decay via (real or virtual) third generation squarks (see Fig. 8) to third generation quarks and EW gauginos. While chargino decay branching fractions tend to follow those of the W -boson, the branching fraction for neutralinos to b quarks is often enhanced in these scenarios. Third generation squarks frequently also have b -quarks as their decay products. Finally, ESUSY events are also often rich in t quarks whose decays contribute to the multi-lepton component of the signal.

We have discussed the phenomenology of five ESUSY benchmark points introduced in Sec. 3.3. Of these, just the point ES3 has a thermal neutralino relic density in accord with the measured cold DM relic density, although here the \tilde{Z}_1 would just make up about 1/3 of the DM. For the other points, the LMP (which need not even be a neutralino) must decay into the true LSP (which might be the axino) plus SM particles. If the LMP is a neutralino, this decay typically occurs well after the neutralino has passed through the LHC detectors, and the LHC phenomenology is essentially the same as for a stable neutralino. The LMP may also be a coloured squark or an electrically charged stau, as illustrated by the last two benchmark points that we discuss. Assuming again that the axino is the LSP, the LMP is quasi-stable and typically traverses the detector before it decays. In these cases, the presence of a (possibly intermittent, in the case of squark LMP) track of a slowly moving particle (whose velocity is

obtained through timing information), rather than E_T^{miss} , will be the hallmark of SUSY events.

To conclude, effective supersymmetry with third generation squarks and EW gauginos at or below the TeV scale, but 10–20 TeV first/second generation sfermions ameliorates the flavour and CP problems that plague many SUSY models. We have examined the LHC phenomenology of relic-density-consistent ESUSY scenarios and shown that it may differ qualitatively from that in the most frequently examined mSUGRA scenario. The ESUSY picture may also be tested in low energy measurements. In particular, if the branching fraction for $B \rightarrow \tau\nu$ decay, and especially the muon magnetic moment show significant deviation from their SM values, the ESUSY picture would be strongly disfavoured.

Acknowledgements

We thank A. Pukhov for his help in implementing the `Isajet – micrOMEGAs` interface for SUSY scenarios with non-universal scalars. XT thanks the UW IceCube collaboration for making his visit to the University of Wisconsin where this work was done, possible. We also thank the Galileo Galilei Institute (GGI), Florence, Italy for hospitality at the time of the Workshop on Dark Matter: Its origin, nature and prospects for detection during which many of the ideas presented in this paper came together. This work was funded in part by the US Department of Energy, and by the French ANR project ToolsDMColl, BLAN07-2-194882.

References

- [1] S. Dimopoulos and H. Georgi, *Nucl. Phys.* **B 193** (1981) 150.
- [2] N. Sakai, *Z. Phys. C*, **11** (1981) 153.
- [3] Y. Nir and N. Seiberg, *Phys. Lett.* **B 309** (1993) 337.
- [4] M. Dine, A. Kagan and S. Samuel, *Phys. Lett.* **B 243** (1990) 250.
- [5] N. Arkani-Hamed and H. Murayama, *Phys. Rev.* **D 56** (1997) R6733.
- [6] M. Drees *Phys. Rev.* **D 33** (1986) 1468.
- [7] S. Dimopoulos and G. Giudice, *Phys. Lett.* **B 357** (1995) 573; A. Pomarol and D. Tomassini, *Nucl. Phys.* **B 466** (1996) 3.
- [8] A. Cohen, D. B. Kaplan and A. Nelson, *Phys. Lett.* **B 388** (1996) 588.
- [9] For an update on $(g - 2)_\mu$, see T. Teubner, K. Hagiwara, R. Liao, A.D. Martn and D. Nomura, arXiv:1001.5401.
- [10] N. Jarosik *et al.*, arXiv:1001.4744 [astro-ph.CO]; E. Komatsu *et al.*, arXiv:1001.4538 [astro-ph.CO].

- [11] R. Peccei and H. Quinn, *Phys. Rev. Lett.* **38** (1977) 1440 and *Phys. Rev.* **D 16** (1977) 1791; S. Weinberg, *Phys. Rev. Lett.* **40** (1978) 223; F. Wilczek, *Phys. Rev. Lett.* **40** (1978) 279.
- [12] H. Baer, A. Box and H. Summy, *J. High Energy Phys.* **0908** (2009) 080; H. Baer and A. Box, arXiv:0910.0333 *Eur. Phys. J.*, in press; H. Baer, A. Box and H. Summy, arXiv:1005.2215 (2010).
- [13] A. Cohen, D. B. Kaplan, F. Lepeintre and A. Nelson, *Phys. Rev. Lett.* **78** (1997) 2300.
- [14] K. Agashe and M. Grassler, *Phys. Rev.* **D 59** (1999) 015007; J. Hisano, K. Kurosawa and Y. Nomura, *Nucl. Phys.* **B 584** (2000) 3.
- [15] J. Bagger, J. Feng, N. Polonsky and R. J. Zhang, *Phys. Lett.* **B 473** (2000) 264.
- [16] H. Baer, P. Mercadant and X. Tata, *Phys. Lett.* **B 475** (2000) 289; H. Baer, C. Balazs, M. Brhlik, P. Mercadante, X. Tata and Y. Wang, *Phys. Rev.* **D 64** (2001) 015002.
- [17] H. Baer and J. Ferrandis, *Phys. Rev. Lett.* **87** (2001) 211803; D. Auto, H. Baer, C. Balazs, A. Belyaev, J. Ferrandis and X. Tata, *J. High Energy Phys.* **0306** (2003) 023; H. Baer, S. Kraml, S. Sekmen and H. Summy, *J. High Energy Phys.* **0803** (2008) 056; H. Baer, S. Kraml and S. Sekmen, *J. High Energy Phys.* **0909** (2009) 005.
- [18] T. Blazek, R. Dermisek and S. Raby, *Phys. Rev. Lett.* **88** (2002) 111804; T. Blazek, R. Dermisek and S. Raby, *Phys. Rev.* **D 65** (2002) 115004; R. Dermisek, S. Raby, L. Roszkowski and R. Ruiz de Austri, *J. High Energy Phys.* **0304** (2003) 037; R. Dermisek, S. Raby, L. Roszkowski and R. Ruiz de Austri, *J. High Energy Phys.* **0509** (2005) 029; W. Altmannshofer, D. Guadagnoli, S. Raby and D. Straub, *Phys. Lett.* **B 668** (2008) 385.
- [19] H. Baer, C. Balazs, P. Mercadante, X. Tata and Y. Wang, *Phys. Rev.* **D 63** (2001) 015011.
- [20] N. Desai and B. Mukhopadhyaya, *Phys. Rev.* **D 80** (2009) 055019; S. G. Kim, N. Maekawa, K. Nagao, M. Nojiri and K. Sakurai, *J. High Energy Phys.* **0910** (2009) 005; N. Bernal, A. Djouadi and P. Slavich, *J. High Energy Phys.* **0707** (2007) 016; N. Bernal, *JCAP***0908** (2009) 022; M. J. White and F. Feroz, arXiv:1002.1922.
- [21] K. L. Chan, U. Chattopadhyay and P. Nath, *Phys. Rev.* **D 58** (1998) 096004; J. Feng, K. Matchev and T. Moroi, *Phys. Rev. Lett.* **84** (2000) 2322 and *Phys. Rev.* **D 61** (2000) 075005; see also H. Baer, C. H. Chen, F. Paige and X. Tata, *Phys. Rev.* **D 52** (1995) 2746 and *Phys. Rev.* **D 53** (1996) 6241; H. Baer, C. H. Chen, M. Drees, F. Paige and X. Tata, *Phys. Rev.* **D 59** (1999) 055014; for a model-independent approach, see H. Baer, T. Krupovnickas, S. Profumo and P. Ullio, *J. High Energy Phys.* **0510** (2005) 020.
- [22] H. Baer and X. Tata, *Weak Scale Supersymmetry: From Superfields to Scattering Events*, (Cambridge University Press, 2006).
- [23] H. Baer, F. Paige, S. Protopopescu and X. Tata, hep-ph/0312045; see also H. Baer, J. Ferrandis, S. Kraml and W. Porod, *Phys. Rev.* **D 73** (2006) 015010. The Isajet manual is available at <http://www.nhn.ou.edu/~isajet/>.

- [24] See H. Baer, A. Mustafayev, S. Profumo, A. Belyaev and X. Tata, *Phys. Rev. D* **71** (2005) 095008 and *J. High Energy Phys.* **0507** (2005) 065, and references therein.
- [25] C. Böhm, A. Djouadi and M. Drees, *Phys. Rev. D* **30** (2000) 035012; J. R. Ellis, K. A. Olive and Y. Santoso, *Astropart. Phys.* **18** (2003) 395; J. Edsjö, *et al.*, *JCAP* **0304** (2003) 001.
- [26] M. Drees and M. Nojiri, *Phys. Rev. D* **47** (1993) 376; H. Baer and M. Brhlik, *Phys. Rev. D* **57** (1998) 567; H. Baer, M. Brhlik, M. Diaz, J. Ferrandis, P. Mercadante, P. Quintana and X. Tata, *Phys. Rev. D* **63** (2001) 015007; J. Ellis, T. Falk, G. Ganis, K. Olive and M. Srednicki, *Phys. Lett. B* **510** (2001) 236; L. Roszkowski, R. Ruiz de Austri and T. Nihei, *J. High Energy Phys.* **0108** (2001) 024; A. Djouadi, M. Drees and J. L. Kneur, *J. High Energy Phys.* **0108** (2001) 055; A. Lahanas and V. Spanos, *Eur. Phys. J. C* **23** (2002) 185.
- [27] G. Belanger, F. Boudjema, A. Pukhov and R. K. Singh, *JHEP* **0911**, 026 (2009) [arXiv:0906.5048 [hep-ph]].
- [28] R. R. de Austri, R. Trotta and L. Roszkowski, *JHEP* **0605**, 002 (2006) [arXiv:hep-ph/0602028].
- [29] B. C. Allanach, K. Cranmer, C. G. Lester and A. M. Weber, *JHEP* **0708**, 023 (2007) [arXiv:0705.0487 [hep-ph]].
- [30] R. Trotta, F. Feroz, M. P. Hobson, L. Roszkowski and R. Ruiz de Austri, *JHEP* **0812**, 024 (2008) [arXiv:0809.3792 [hep-ph]].
- [31] F. Mahmoudi, *Comput. Phys. Commun.* **180**, 1579 (2009) [arXiv:0808.3144 [hep-ph]].
- [32] G. Belanger, F. Boudjema, A. Pukhov and A. Semenov, *Comput. Phys. Commun.* **176**, 367 (2007) [arXiv:hep-ph/0607059].
- [33] O. Buchmueller *et al.*, *Eur. Phys. J. C* **64**, 391 (2009) [arXiv:0907.5568 [hep-ph]].
- [34] E. Barberio *et al.* [Heavy Flavor Averaging Group], arXiv:0808.1297 [hep-ex].
- [35] M. Misiak *et al.*, *Phys. Rev. Lett.* **98**, 022002 (2007) [arXiv:hep-ph/0609232].
- [36] T. Aaltonen *et al.* [CDF Collaboration], *Phys. Rev. Lett.* **100**, 101802 (2008) [arXiv:0712.1708 [hep-ex]].
- [37] Tevatron Electroweak Working Group (CDF and D0 collaborations), arXiv:0903.2503 [hep-ex].
- [38] LEP2 SUSY Working Group (ALEPH, DELPHI, L3 and OPAL collaborations), <http://lepsusy.web.cern.ch/lepsusy/>
- [39] T. E. W. Group [CDF Collaboration and D0 Collaboration], arXiv:0908.2171 [hep-ex].
- [40] H. Baer and H. Summy, *Phys. Lett. B* **666**, 5 (2008) [arXiv:0803.0510 [hep-ph]].

- [41] A. Box and X. Tata, *Phys. Rev. D* **79** (2009) 035004.
- [42] L. Covi, J. E. Kim and L. Roszkowski, *Phys. Rev. Lett.* **82** (1999) 4180; L. Covi, H. B. Kim, J. E. Kim and L. Roszkowski, *J. High Energy Phys.* **0105** (2001) 033.
- [43] A. Brandenburg *et al.* *Phys. Lett. B* **617** (2005) 99.
- [44] L. Covi, L. Roszkowski and M. Small, *J. High Energy Phys.* **0207** (2002) 023.
- [45] K. Jedamzik, *Phys. Rev. D* **74** (2006) 103509.
- [46] A. Freitas, F. Steffen, N. Tajuddin and D. Wyler, *Phys. Lett. B* **682** (2009) 193.
- [47] C. Berger, L. Covi, S. Kraml and F. Palorini, *JCAP***0810** (2008) 005.
- [48] U. Chattopadhyay, A. Datta, A. Datta, A. Datta, and D. P. Roy, *Phys. Lett. B* **493** (2000) 127; P. Mercadante, J. K. Mizukoshi and X. Tata, *Phys. Rev. D* **72** (2005) 035009; S. P. Das, A. Datta, M. Guchait, M. Maity and S. Mukherjee, *Eur. Phys. J. C* **54** (2008) 645; R. Kadala J. K. Mizukoshi, P. Mercadante and X. Tata, *Eur. Phys. J. C* **56** (2008) 511.
- [49] H. Baer, S. Kraml, S. Sekmen and H. Summy, *J. High Energy Phys.* **0810** (2008) 079; H. Baer, S. Kraml, A. Lessa and S. Sekmen, *J. High Energy Phys.* **1002** (2010) 055.
- [50] H. Baer, X. Tata and J. Woodside, *Phys. Rev. D* **42** (1990) 1568.
- [51] H. Baer, C. H. Chen, F. Paige and X. Tata, *Phys. Rev. D* **50** (1994) 4508.
- [52] H. Baer, S. Kraml, S. Sekmen. *J. High Energy Phys.* **0909** (2009) 005
- [53] I. Hinchliffe *et al.* *Phys. Rev. D* **55** (1997) 5520 and *Phys. Rev. D* **60** (1999) 095002; H. Bachacou, I. Hinchliffe and F. Paige, *Phys. Rev. D* **62** (2000) 015009.
- [54] H. Baer, V. Barger, G. Shaughnessy, H. Summy and L. T. Wang, *Phys. Rev. D* **75** (2007) 095010.
- [55] C. Lester and D. Summers, *Phys. Lett. B* **463** (1999) 99; A. Barr, C. Lester and D. Summers, *J. Phys. G***29** (2003) 2343; W. S. Cho, K. Choi, Y. Kim and C. Park, *Phys. Rev. Lett.* **100** (2008) 171801 and *J. High Energy Phys.* **0802** (2008) 035; H-C. Cheng and Z. Han, *J. High Energy Phys.* **0812** (2008) 063.
- [56] C. Lester and a Barr, *J. High Energy Phys.* **0712** (2007) 102; B. Gripaios, *J. High Energy Phys.* **0802** (2008) 053; A. Barr, B. Gripaios and C. Lester, *J. High Energy Phys.* **0911** (2009) 096; K. Matchev, F. Moortgat, L. Pape and M. Park, *J. High Energy Phys.* **0908** (2009) 104.
- [57] R. Kadala *et al.* Ref.[48].
- [58] J. Hisano, K. Kawagoe and M. Nojiri, *Phys. Rev. D* **68** (2003) 035007; J. Hisano, K. Kawagoe, R. Kitano and M. Nojiri, *Phys. Rev. D* **66** (2002) 115004.

- [59] S. Kraml and A. R. Raklev, *Phys. Rev.* **D 73** (2006) 075002.
- [60] A. Heister *et al* (ALEPH Collaboration), *Eur. Phys. J.* **C 31** (2003) 327.
- [61] T. Aaltonen *et al.* (CDF Collaboration), arXiv:0902.1266.
- [62] A. Raklev, arXiv:0908.0315.
- [63] M. Fairbairn *et al.*, *Phys. Rept.* **438** (2007) 1.
- [64] M. Drees and X. Tata, *Phys. Lett.* **B 252** (1990) 695.
- [65] H. Baer, K. Cheung and J. Gunion, *Phys. Rev.* **D 59** (1999) 075002.
- [66] G. Abbiendi *et al.* (OPAL Collaboration), *Phys. Lett.* **B 572** (2003) 8.